



Universiteit Utrecht

Comparing P and S wavespeed perturbations for the mantle beneath Europe



K. Visser ⁽¹⁾ and R.D. van der Hilst ^(1,2)

(1) Utrecht University, department of Seismology, kvis@geo.uu.nl

(2) Massachusetts Institute of Technology (MIT), Earth, Atmospheric, and Planetary Sciences

Introduction

P and *S* wavespeed perturbation models for Europe are constructed using a selected part of the EHB dataset. We selected events where both a *P* (or *PP*) and a *S* (or *SS*) delay time were available for one event and one station. The resulting model has similar ray coverage for *P* and *S* and, hence, similar resolution properties. The bulk sound speed, Poisson's ratio and $R = \partial \ln V_s / \partial \ln V_p$ are extracted from these models.

Data

The data selection restricts severely the number of data that may be used for inversion. In total, we selected 714.412 *P* and *S* pairs and 27.274 *PP* and *SS* pairs. An irregular grid was used with smaller cell sizes in the region of interest (Europe). The *P* and *S* wave data are inverted separately through an iterative conjugate gradient algorithm to obtain the *P* and *S* wavespeed perturbation models.

Synthetic tests

To test the joint inversion we used a checkerboard test for the *P*, *S* and Poisson's ratio perturbations. The shape of the checkerboard corresponds to the input model, especially in regions where the sampling is dense. The amplitude of the *P* and *S* wavespeed anomalies is only about 25% of the input model, whereas the amplitudes of the Poisson's ratio is almost completely recovered. As expected, the resolution for the separate *P* and *S* wavespeed perturbation models is lower both compared to inversions that use the whole EHB dataset and to the relative variations of the *P* and *S* wavespeed perturbations.

Results

A positive but decreasing correlation was found for the *P* and *S* wavespeed perturbations up to 1500 km (Figure 2). The bulk sound speed is not significantly correlated to the shear wave speed in most of the mantle, except in the transition zone where the bulk sound speed appears to be negatively correlated to the shear wave speed. Figure 3 shows *R* for different regions.

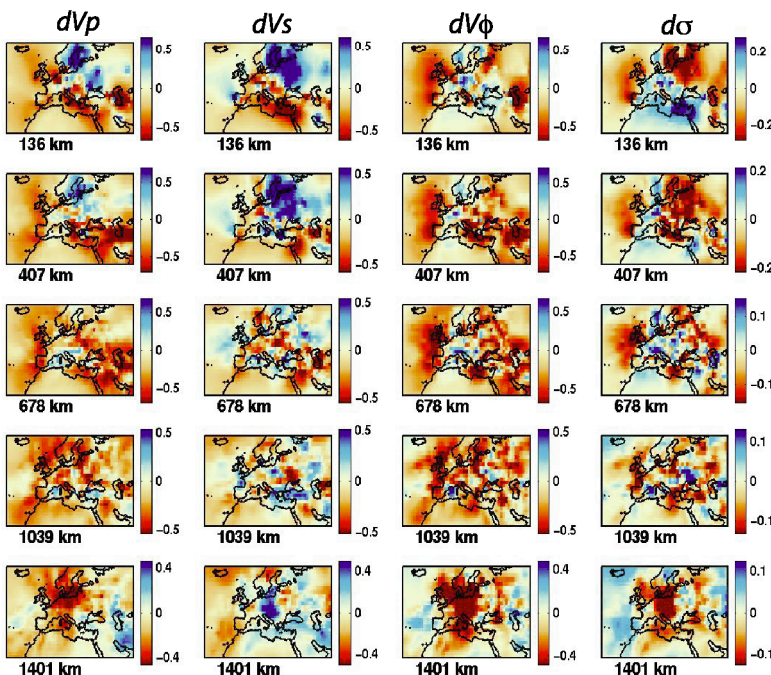


Figure 2. Correlation between the bulk sound speed anomalies and the shear wavespeed anomalies ($dVs-dV\phi$) and the correlation between the *P* wavespeed perturbations versus the *S* wavespeed perturbations ($dVs-dVp$). We consider the correlation coefficient to be insignificant if they fall within the grey area.

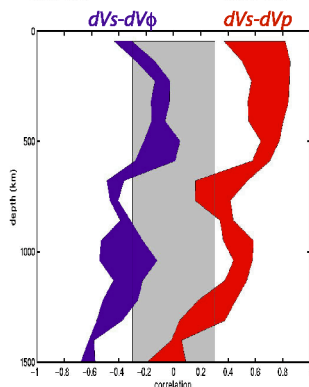


Figure 1. Perturbations in *P*-wave, *S*-wave, bulk sound speed and Poisson's ratio in percent for the five given depths.

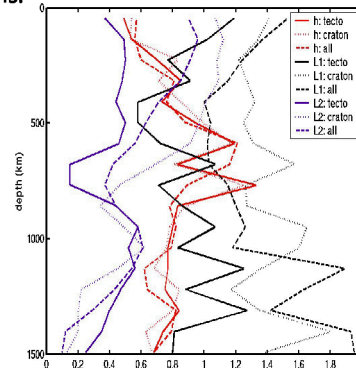


Figure 3. *R* as a function of depth for different regions (the tectonic, cratonic and the whole of Europe) and different methods. *R* is measured in two different ways. The first method is a line fitting (L1- or L2-norm) in a dVs against dVp plot. The second method makes use of histograms (h) representing the distribution of values obtained.

Conclusions

We find small values of *R* between 0.4 and 1.5, that do not vary significantly from region to region. Values of *R* between 1.0 and 2.0 can be explained with thermal effects. Values outside this region cannot be explained using thermal effects alone. The perturbation in the Poisson's ratio is most striking at shallow depths for the cratonic and tectonic part of Europe. More good quality data is needed to obtain more details about the behaviour of the Poisson's ratio and *R* in the mantle beneath Europe.